Journal of Colloid and Interface Science 434 (2014) 201–207

Contents lists available at ScienceDirect

Journal of Colloid and Interface Science

www.elsevier.com/locate/jcis

Self-assembly of the triblock copolymer 17R4 poly(propylene oxide)$_{14}$–poly(ethylene oxide)$_{24}$–poly(propylene oxide)$_{14}$ in D_2O

Bryna C. Kumi [a,*], Boualem Hammouda [b], Sandra C. Greer [a,c,1]

[a] Department of Chemistry and Biochemistry, The University of Maryland, College Park, College Park, MD 20742, United States
[b] Center for Neutron Research, National Institute of Standards and Technology, Gaithersburg, MD 20899, United States
[c] Department of Chemical and Biomolecular Engineering, The University of Maryland, College Park, College Park, MD 20742, United States

ARTICLE INFO

Article history:
Received 5 June 2014
Accepted 29 July 2014
Available online 12 August 2014

Keywords:
Micelles
Block copolymers
SANS
Poly(propylene oxide)–poly(ethylene oxide)–poly(propylene oxide)

ABSTRACT

Our recent investigation of the three regions of the phase diagram of 17R4 in D_2O (Huff et al., 2011) has led us to study the copolymer structure in this system by small-angle neutron scattering, rheometry, and dynamic light scattering. In region I at low temperatures and copolymer concentrations (0–30 °C, 0.1–0.2 mass fraction ω), the cloudy solution contains the copolymer in large clusters made of hydrophobic PPO-rich "knots" bridged by dissolved hydrophilic PEO chains. These clusters vanish in region I at the lower temperatures and concentrations (below 39 °C and $\omega = 0.01$). In region I over long times (weeks) at 25 °C, a white liquid/gel film forms at the air–D_2O interface. In region II at temperatures above the micellization line (above about 35 °C, at $\omega = 0.22$) the large clusters dissipate and unimers coexist with "flower micelles," where the PPO blocks are the centers of the micelles and the PEO blocks loop into the solvent. In region III at still higher temperatures (above about 40 °C at $\omega = 0.2$), the solution separates into coexisting liquid phases, where the upper phase of higher copolymer concentration is in region II, and the lower phase is in region I. The concentrated upper phase may contain micelles so crowded as to form a network.

© 2014 Elsevier Inc. All rights reserved.

1. Introduction

Reverse Pluronic 17R4 is a triblock copolymer consisting of two end blocks of poly(propylene oxide) (PPO) with a middle block of poly(ethylene oxide) (PEO): PPO_{14}–PEO_{24}–PPO_{14}, where the subscripts indicate the number of monomers in each polymer block. Thus the end blocks are hydrophobic and the center block is hydrophilic, allowing for possibilities of self-assembly in water. The phase diagrams of 17R4 in H_2O and in D_2O [1,2] show micellization lines intersecting liquid–liquid phase separations with lower critical solution points. In Fig. 1, region I is termed the "cloudy" region because the solution is cloudy in appearance, region II is termed the "clear" region because the solution is transparent, and region III is the region of coexistence of two liquid phases. The line that separates region I and region II is the micellization line, and there is evidence of micelle formation in region II for H_2O solutions [2,3]. The boundary of the two-phase region III in Fig. 1 is a "cloud point curve" drawn from the appearance either of cloudiness indicating the incipient phase separation or of an actual second phase. Because of the polydispersity of the copolymer solute, the cloud point curve is not the same as a true coexistence curve [1,4].

The development of this interesting phase diagram, one that combines self-assembly with a lower critical solution point and a phase separation, motivated us to try to understand the changes in microscopic structure that cause the phase changes. We have found that in region I at the very lowest temperatures and mass fractions, the copolymer molecules (unimers) are unassociated, but as temperature and mass fraction increase, some of the copolymers associate into networks or clusters of large dimension (>200 Å). We propose that the clusters are groups of hydrophobic PPO blocks, connected by hydrophilic PEO chains [5]. In region II, the large clusters disappear and small (~30 Å) micelles form that are necessarily "flower" micelles, where the PPO blocks cluster in the core and the PEO blocks loop into the solvent [5,6]. In the two-phase region III, the upper phase of higher copolymer concentration is in region II, and the lower phase is in region I. The high concentration of the upper phase may force the micelles into a micellar network with some unimers shared by micelles.

* Corresponding author. Present address: Department of Chemistry and Biochemistry, Rowan University, Glassboro, NJ 08028, United States.
E-mail address: bryna.kumi@gmail.com (B.C. Kumi).
[1] Present address: Department of Chemistry, Mills College, Oakland, CA 94613, United States.

http://dx.doi.org/10.1016/j.jcis.2014.07.049
0021-9797/© 2014 Elsevier Inc. All rights reserved.

2. Materials and methods

2.1. Sample preparation

The 17R4 sample, PPO_{14}–PEO_{24}–PPO_{14}, was the same material used by Huff et al. [1]. The manufacturer BASF Corporation reported an average molecular mass of 2650 g/mol and a mass density (ρ) of 1.048 g/mL. Size exclusion chromatography showed a single peak with a number average molecular mass of 2670 g/mol and a polydispersity index of 1.06 [7]. The copolymer was used as received. Three sample concentrations were selected that would to allow us to study the three regions of the phase diagram as temperature was varied: $\omega = 0.0095$, 0.11, and 0.023.

Deuterium oxide (D_2O, 99.9%, $\rho = 1.10$ g/mL at 20–50 °C [8]) was obtained from Cambridge Isotopes, Inc. Solutions were prepared by massing (±0.1 mg; buoyancy corrections applied [9]) the copolymer and the solvent into glass vials with Teflon-lined lids and shaking to mix.

2.2. Rheometry and dynamic light scattering (DLS) methods

An AR 2000 stress-controlled rheometer (TA Instruments, Newark, DE) with cone-and-plate geometry was used: 400 mm diameter, 1°58′47″ cone angle, 47 μm between cone and plate.

DLS measurements and analysis were made as described previously [10,11]. Analysis required the shear viscosity, measured by rheometry (as above), and the refractive index of D_2O [12]. The correlation function was fitted using DynaLS version 2.8.3 (Alango Ltd.). Data at low channel numbers were omitted due to irregular scatter and data at high channel numbers were excluded where the autocorrelation function had decayed to a "foot" or the baseline [7].

The peak position is reported as the hydrodynamic radius value (R_h), but the standard deviation of R_h is overestimated by DynaLS [13]. The uncertainty in R_h was estimated by propagation of error for one sample that showed a single type of scattering body and was found to be 10%. The R_h values reported are the averages of at least four repetitions, with uncertainties obtained by the propagation of 10% error from each repetition [7].

2.3. Small-angle neutron scattering (SANS) methods

SANS measurements were taken at the National Institute of Standards and Technology Center for Neutron Research in Gaithersburg, MD, on the NG3 30-m instrument [14]. Samples were placed in titanium cells with quartz crystal windows and 1 mm sample path lengths, in a temperature-controlled sample holder. Samples were allowed one hour to equilibrate at each temperature. Three sample-to-detector distances were used (1.33, 4.00, and 13.17 m) with a neutron beam wavelength λ of 6 Å to obtain a Q range of (0.003433–0.461) $Å^{-1}$, where the scattering wave vector $Q = (4\pi/\lambda)\sin(\theta/2)$ and θ is the scattering angle. The scattered intensity $I(Q)$ was obtained by circular averaging of the intensity. Typical empty cell and blocked beam corrections were made. Averaged data were placed on an absolute cross-sectional scale.

Linear Guinier ($\ln(I)$ vs Q^2) and Porod ($\log(I)$ vs $\log(Q)$) plots give particle dimensions and determine scaling exponents [15–19]. For each scattering entity, $I(Q)$ is described by scaling exponent n, Q^{-n}, for the Guinier region, or m for the Porod region. At low Q, spherical scatterers show no dependence on Q: $n = 0$. At intermediate Q, the exponent indicates particle dimension: $n = 2$ for plates, $n = 1$ for cylinders or rods. A peak at intermediate Q can indicate interparticle interactions and its position will correspond to the average distance between particles.

At high Q, the Porod scaling exponents are $m = 3$ for a particle with a rough surface, or $m = 4$ for a smooth surface [15]. Mass fractals, particles without a distinct surface from which to scatter, show m between 1 and 3: $m = 1$ for scattering from a one-dimensional object (e. g., a rigid rod), $m = 2$ for a Gaussian coil, and $m = 3$ for a very dense particle. Mass fractal particles include swollen polymers ($m = 5/3$) and collapsed polymers ($m = 3$) [15]. Thus a highly collapsed mass fractal scatters as a rough surface fractal, both having $m = 3$.

Non-linear fits were made to the correlation length model [15] and the Guinier–Porod model [20]. The correlation length model is [15]:

$$I(Q) = \frac{A}{Q^{m_c}} + \frac{C}{1 + (Q\xi)^{m_u}} + B, \tag{1}$$

where m_c is the Porod exponent of the cluster, m_u is the Porod exponent of the unimer, B is the background scattering, and ξ is the correlation length.

The Guinier–Porod model uses a Guinier function:

$$I(Q) = \frac{G}{Q^n}\exp\left(\frac{-Q^2R_g^2}{3-n}\right) + B \quad \text{for } Q \le Q_1, \tag{2}$$

and a Porod function:

$$I(Q) = \frac{D}{Q^m} + B \quad \text{for } Q \ge Q_1, \tag{3}$$

where

$$Q_1 = \frac{1}{R_g}\sqrt{\frac{(m-n)(3-n)}{2}}. \tag{4}$$

Here n is the exponent at intermediate Q scattering for a given scatterer, m is the Porod exponent at high-Q for a given scatterer, B is the background scattering, and G is a fitted scale constant.

3. Results and discussion

All uncertainties are given at the 99.7% confidence level (three times the standard deviation), unless otherwise noted. Details of fits are given in Supplementary Information.

3.1. Surface layer formation in region I

All the samples of 17R4 in D_2O were prepared, sealed, and observed over time at room temperature, in region I. One sample at $\omega = 0.23$ was observed over time in a water bath at (25.52 ± 0.01) °C and showed the same behavior as the samples at room temperature.

The samples were initially cloudy. Over one to two weeks, the cloudiness began to clear, starting from the bottom and moving toward the liquid–air interface, but the samples still remained hazy near the bottom and cloudier near the interface (Supplementary Information, Fig. S1). During this time, a white, opaque, gel-like film collected at the liquid–air interface. We were not able to estimate the amount of copolymer material in the surface film. While we did not deliberately investigate the formation of the film when samples were in regions II and III, we never observed the film except in region I. This surface film has not been studied in 17R4 in H_2O [1]. Zhou and Chu [2] reported cloudiness in 17R4/H_2O and found that it was eliminated by filtering the samples. Similarly, studies of homopolymer poly(ethylene oxide) in D_2O showed that filtering decreases cloudiness by breaking up assemblies of the polymer [21]. We found that filtering the solutions with a 0.2 μm pore filter had little effect either on the degree of cloudiness of

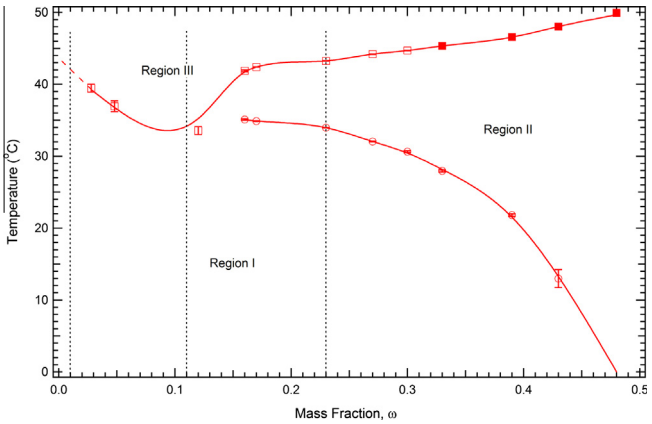

Fig. 1. Phase diagram of 17R4 in D_2O [1]. The transition between the cloudy (I) and clear (II) regions is shown with circles. The transition between the one-phase regions (I and II) and the two-phase region (III) is shown with squares. Open squares signify observation of meniscus formation; closed squares signify observation of a cloud-point. Some error bars, representing three standard deviations, are smaller than the symbols. Lines are drawn through the data points to guide the eye; the dashed line at the left is an extrapolation. Vertical dotted lines indicate the 17R4 mass fractions at which the copolymer structure is studied here: $\omega = 0.0095$, 0.11, and 0.23. The true critical composition is 0.22 ± 0.01 in volume fraction or mass fraction [1].

17R4 in D_2O or in H_2O [1], or on the formation of surface layers in D_2O [7].

This surface film is an interesting phenomenon that we did not pursue further. There are prior studies of the surface activity of PEO–PPO–PEO triblock copolymers [22,23], but we are aware of no studies on PPO–PEO–PPO systems such as 17R4. We might expect more dramatic surface behavior, since the PPO–PEO–PPO copolymer is more hydrophobic than is PEO–PPO–PEO. In addition, hydrophobic effects will be stronger in D_2O than in H_2O [24–26].

The long time (weeks) for film formation could indicate very long times to true equilibrium in these copolymer solutions. Data on the phase diagram of this system were taken on the time scale of one to three hours, before the onset of film formation [1]. The new data discussed here were also taken at one to three hours. A study of the reversibility of structure formation (see Section 3.3.2 below) indicated that the structures were formed and broken within one to three hours.

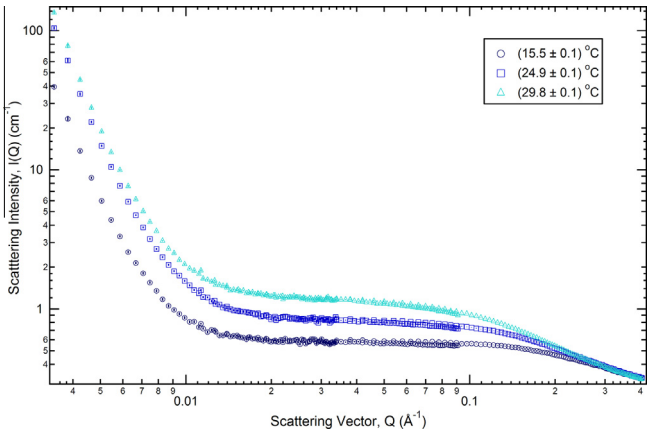

Fig. 2. SANS data from $\omega = 0.23$ 17R4 in D_2O in region I. Error bars, indicating one standard deviation, are smaller than the plotting symbols. Strong scattering at low Q indicates the presence of large clusters at all temperatures.

3.2. Structure in region I

DLS was not used in region I because the sample cloudiness precluded the transmission of light. SANS was used at the three mass fractions indicated by vertical lines in Fig. 1, and rheometry was used at $\omega = 0.23$.

The zero-shear viscosity for the sample at $\omega = 0.23$ is (12.5 ± 0.5) cP at 25 °C and (12.4 ± 0.5) cP at 30 °C [7]. For comparison, the shear viscosity of pure D_2O at 30 °C is 0.969 cP [8], and (see Section 3.3) the viscosity of this copolymer solution in region II is (10.3 ± 0.3) cP.

3.2.1. SANS for $\omega = 0.23$ and $\omega = 0.11$ 17R4/D_2O in region I

For the $\omega = 0.23$ sample, SANS data were collected at three temperatures in region I. Fig. 2 shows that at 29.8 °C and below, there is very strong scattering at low Q and weak scattering at high Q. The strong low-Q scattering indicates the presence of large structures: clusters. The weak scattering in the mid-to-high Q range indicates interactions between copolymer and solvent. An increase of the intermediate-Q intensity upon heating (Fig. 2) portends that a phase separation occurs upon heating. The very high-Q scattering shows m to be about 2, corresponding to free unimers and/or to unimers bridging between PPO groups in clusters (see below).

In order to perform linear analyses on scattering from the unimers, scattering intensity from the background and the clusters had to be removed. The correlation length model fits both cluster and unimer scattering data via Eq. (1) and was used before the linear analyses in order to determine and subtract the cluster and background scattering. The Guinier–Porod model was used (Eqs. 2–4), with a limited Q range of (0.017–0.40) Å^{-1} to exclude cluster scattering and with exponent n fixed at zero to assume spherical unimer conformations. Results are given in Table 1 and discussed below. Note that in region I, m_c for clusters is about 3.6 (three-dimensional scatterer with a smooth surface), m_u for unimers is about 2 (Gaussian coil), and R_g for the unimer is less than or near to 10 Å.

Fig. 3 shows that for $\omega = 0.11$ at 11.9 °C and 30.6 °C, the scattering is like that seen in region I for $\omega = 0.23$, indicating the presence of clusters along with unimers. The $\omega = 0.11$ data were analyzed using the correlation length model and the results in Table 1 are consistent with results for $\omega = 0.23$ in region I. The data at 49.3 °C, in region III, are discussed below in Section 3.3.

Such strong low-Q scattering has been seen in many similar systems, including synthetic polymers and biopolymers in D_2O [21,27–31]. The exact structure of such "clusters" is unknown, but work on PEO in D_2O [27] and on the Reverse Pluronic 25R8 in D_2O [31] offer insight. PEO in D_2O forms clusters by interactions among ethylene groups of separate chains [27]. Although PEO does dissolve in water, the hydrophobic ethylene groups minimize interaction with the solvent by residing near other ethylene groups, causing the chains to cross-link physically and to form a cluster network. The clusters in PEO have $m_c = 3$, indicating a mass fractal and a rough surface fractal. The clusters in 17R4/D_2O may be different, since m_c is about 3.6 (Table 1), indicating a more solid object and a smoother surface.

Reverse Pluronic 25R8 is PPO_{15}–PEO_{156}–PPO_{15} and has a PEO block that is about seven times larger than in 17R4. In 25R8/D_2O solutions [31], it has been suggested that the hydrophobic PPO blocks group together to form "knots," while the PEO blocks extend into solution. SANS from these 25R8 structures shows $m_c = 4$, indicating a smooth surface fractal. Such a structure seems plausible for 17R4 in D_2O, as shown in Fig. 4 [5]. Because scattering from the 17R4 clusters extends beyond the SANS window, it is not possible to determine their size, except to say that at $\omega = 0.23$ the clusters are larger than 6000 Å, the limit of the SANS technique [15].

Table 1
Results of SANS and DLS analyses for 17R4 in D_2O. Here (u) indicates unimer, (m) micelle, and (c) cluster. Porod exponents are for clusters (m_c) and unimers (m_u). For $\omega = 0.23$, m_c values are from the correlation length model, m_u values are from linear Porod fits, and R_g values are averages from the correlation length model, linear Guinier fits, and Guinier–Porod model results (see Supplementary Information, Tables S1 and S2). R_h values are from DLS analysis. For $\omega = 0.11$, all values are from the correlation length model. For $\omega = 0.0095$, all values are from the Guinier–Porod model. Statistical uncertainties correspond to three standard deviations.

ω	Region	T (°C)	m_c	m_u	R_g (Å)	R_h (Å)
0.23	I	15.5 ± 0.1	3.52 ± 0.03	2.23 ± 0.12	5.5 ± 0.2 (u)	
	I	24.9 ± 0.1	3.59 ± 0.03	2.08 ± 0.10	7.8 ± 0.1 (u)	
	I	29.8 ± 0.1	3.60 ± 0.02	1.97 ± 0.07	10.58 ± 0.2 (u)	
	II	35 ± 1				2.8 ± 0.1 (u)
					31.02 ± 0.06 (m)	30 ± 4 (m)
	II	40 ± 1				4.9 ± 0.2 (u)
					31.91 ± 0.03 (m)	29 ± 1 (m)
0.11	I	11.9 ± 1.0	3.20 ± 0.05	2.42 ± 0.07	7.8 ± 0.1 (u)	
	I	30.6 ± 1.1	3.59 ± 0.03	2.11 ± 0.03	13.06 ± 0.07 (u)	
0.0095	I	11.9 ± 1.0	na	1.2 ± 0.1	12.5 ± 0.8 (u)	
	I	21.3 ± 1.0	na	1.2 ± 0.1	12.5 ± 0.8 (u)	
	I	30.6 ± 1.1	na	1.3 ± 0.1	11.3 ± 0.7 (u)	
	I	39.9 ± 1.2	Fixed at 4.0	1.5 ± 0.2	9.8 ± 0.6 (u)	
					220 ± 40 (c)	

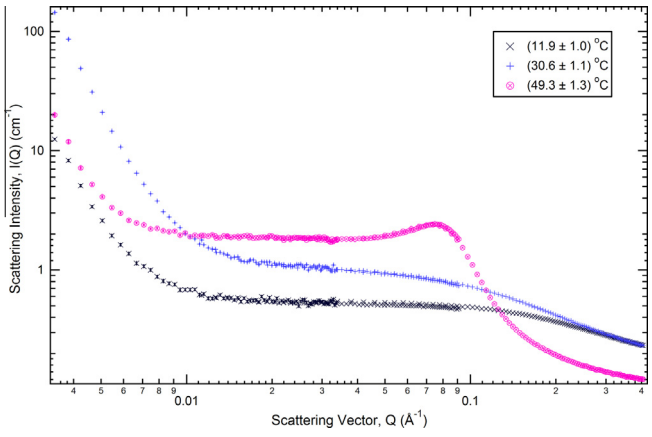

Fig. 3. SANS data from $\omega = 0.11$ 17R4 in D_2O in region I (11.9 °C and 30.8 °C) and in region III (49.3 °C). Scattering from unimers or unimers bridging between clusters (high Q) and from clusters (low Q) appear at all temperatures. At 49.3 °C, the peak indicates that phase separation has occurred. Error bars indicate one standard deviation.

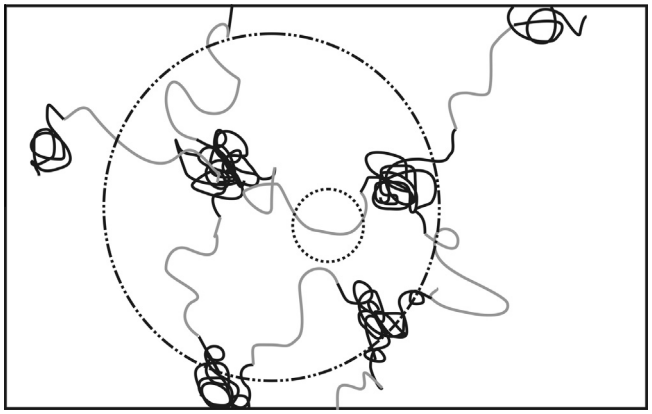

Fig. 4. Proposed clustering of unimers in 17R4/D_2O solutions in region I. PPO is shown in black and PEO is in gray. A cluster is shown within the large, dashed and dotted (–··–··–) circle, corresponding to scattering from low-Q dimensions. A unimer chain section is shown within the small, dotted circle, corresponding to scattering from high-Q dimensions.

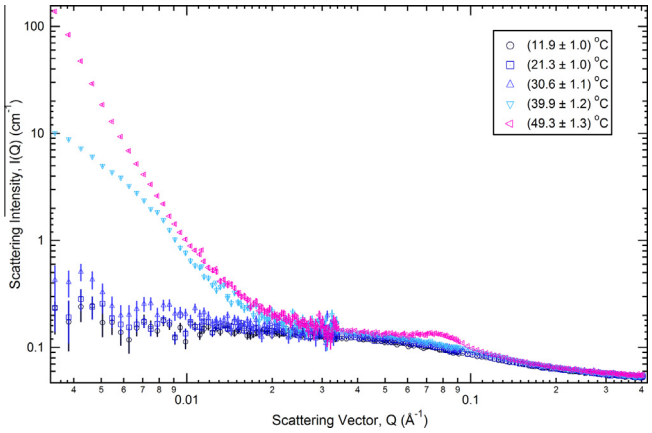

Fig. 5. SANS data from $\omega = 0.0095$ 17R4 in D_2O. Unimer scattering is apparent in region I (11.9, 21.3, 30.6) °C, cluster scattering appears at and above 39.9 °C, and a peak indicating phase separation in region III appears at 49.3 °C. Error bars correspond to one standard deviation.

We assume that this clustering causes the turbidity in 17R4/D_2O samples in region I. Although clustering is seen in PEO/D_2O samples, no cloudiness has been reported in that system. The cloudiness in 25R8/D_2O and 17R4/D_2O systems can be due to larger "knots" of PPO blocks, versus the individual ethylene groups in PEO/D_2O solutions.

Fig. 4 also depicts a high-Q window and a portion of the cluster structure that corresponds to scattering at high Q. Solvated PEO blocks stretched between PPO "knots" will scatter in a manner similar to free unimers in solution and scattering from the two cannot be distinguished. These are "apparent" radii because the fitting models do not account for interparticle interactions. Because the radii are so small, this scattering is near the SANS detection limit, and it is only possible to say that these scattering bodies have a size of less than 10 Å. There is a seeming increase in R_g with increasing temperature (Table 1), in contrast to a slight decrease in R_h seen in 17R4/H_2O [2], but the changes are below the SANS detection limit and do not warrant interpretation.

3.2.2. SANS for $\omega = 0.0095$ 17R4/D_2O in region I

Scattering at $\omega = 0.0095$ in region I differed from that at the higher concentrations (Fig. 5). At the three lowest temperatures, no significant scattering occurred at low Q, indicating that clusters are absent. Unimer R_g values from the Guinier–Porod model, in

Table 1, are consistent with those for the more concentrated samples, but m_u is near 1.3, indicating a very open mass fractal for the unimers. These fits also gave intermediate exponents n_u of 0.18–0.27, almost $n = 0$, indicating a nearly spherical scatterer.

At 39.9 °C, low-Q scattering from clusters appeared. These clusters were smaller than those at the higher mass fractions, with $n_c = 0.9 \pm 0.3$ and $n_u = 0.39 \pm 0.04$, indicating a slightly anisotropic cluster and a nearly spherical unimer. The R_g of the cross-section of the cluster fell within the SANS window at about 220 Å. As the R_g of the clusters did not fall within the SANS window at the higher mass fractions, it follows that the dimensions of the clusters grow with increased mass fraction.

3.2.3. Summary for region I

At low mass fractions and temperatures, 17R4 in D_2O exists as free unimers that are spherical in conformation with an R_g of 10 Å or less. As the mass fraction or the temperature increases, large clusters appear and grow in size. We propose that the clusters form as the insoluble PPO blocks group together to avoid D_2O interactions, while the PEO blocks continue to be hydrated in the solvent [5]. The sizes of the clusters are above the range of the SANS analysis, except for the sample at the lowest mass fraction, where a dimension of about 200 Å was determined for an asymmetric cluster geometry.

3.3. Structure in region II

Solutions $\omega = 0.0095$ and $\omega = 0.11$ did not show region II, but upon increase of temperature moved directly from region I to region III (Fig. 1). Only the $\omega = 0.23$ sample exhibited region II, and the transition from the cloudy solution in region I to the clear solution in region II happened in an hour or two.

The zero-shear viscosity of $\omega = 0.23$ 17R4/D_2O solution was measured to be 10.3 cP ± 0.3 cP at both 35 °C and 40 °C. Thus the zero-shear viscosity is 18% less in region II than in region I. This suggests that there are more interactions and connectivities among copolymers in region I than in region II.

DLS showed two species in region II: the free unimers and a larger species that we assume to be flower micelles (see below) [5]. R_h values are given in Table 1, the unimers at 3–5 Å and the micelles at about 30 Å. The R_h values of the unimers from DLS in region II are of the same magnitude as the R_g values obtained from SANS in region I and in region II (see below). R_h for the unimers nearly doubles between 35 °C and 40 °C, but we hesitate to interpret this change, given that these sizes are near the DLS detection limit.

3.3.1. SANS from $\omega = 0.23$ 17R4/D_2O in region II

Fig. 6 shows the SANS data from the $\omega = 0.23$ 17R4/D_2O solution at 29.8 °C (region I), 34.5 °C (region II) and 39.2 °C (region II). The data in region II do not show high intensity scattering at low Q, an important difference from the scattering in region I and evidence that the large clusters present in region I have been disrupted in region II. The disappearance of the clusters is abrupt, in contrast to the system 25R8/D_2O [31], where cluster scattering was observed well into the micelle region and was taken to indicate a micellar network.

In region II, scattering intensity reaches its maximum at the mid-Q range, suggesting scatterers of moderate size, like the micelles seen by DLS. The micelles are nearly spherical, as there is little Q-dependence at low Q. Scattering intensity grows as temperature increases in region II, suggesting an increase in the number of micelles.

The correlation length model was used to estimate the background scattering, with the coefficient for the cluster term (A in Eq. (1)) set to zero, since no clusters exist in region II. Then R_g values from three methods of SANS data analysis are in agreement (Supplementary Information, Table S2) and their averages can be compared to the R_h values from DLS analyses (Table 1).

The radius of about 30 Å measured for the micelles may seem small, but generally the radii for micelles in Reverse Pluronics are smaller than in regular Pluronics. For example, the Pluronic L64, $PEO_{13}PPO_{30}PEO_{13}$, in H_2O has a micelle R_h of about 60 Å, [2,32,33], and the Pluronic L44, $PEO_{10}PPO_{23}PEO_{10}$, in H_2O has a micelle R_h of 72 Å [34]. On the other hand, Reverse Pluronic 10R5, $PPO_8PEO_{22}PPO_8$, in H_2O has a micelle R_h of 16 Å [34], and 17R4 itself in H_2O has a micelle R_h of about 40 Å [2]. Thus the micelle radius for 17R4 in D_2O is consistent with dimensions seen for other Reverse Pluronics in H_2O, where they form "flower micelles." Flower micelles can form when the solvent is a good solvent for the middle block of the copolymer and a poor solvent for the end blocks, so that the end blocks (here, PPO) are in the core of the micelle and the middle block (PEO) loops into the solvent. Flower micelles require a loss of entropy to loop the middle blocks into the solvent and thus can be expected to be smaller than core-shell micelles [5].

Porod exponents for the micelles, m_m, are around 2 at 34.5 °C and near 3 at 39.2 °C (Table S3, Supplementary Information) and indicate a very dense mass fractal at 34.5 °C and a very rough surface fractal near 40 °C, supporting the presence of flower micelles with loose, solvated "petals" at 34.5 °C and more compact "petals" at 39.2 °C.

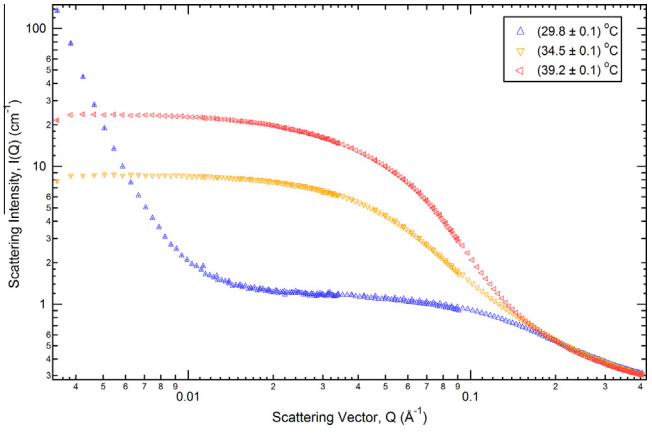

Fig. 6. SANS data from $\omega = 0.23$ 17R4 in D_2O in region II at 34.5 °C and 39.2 °C. Region I scattering at 29.8 °C is also shown. Region II scattering does not show the low-Q scattering of clusters.

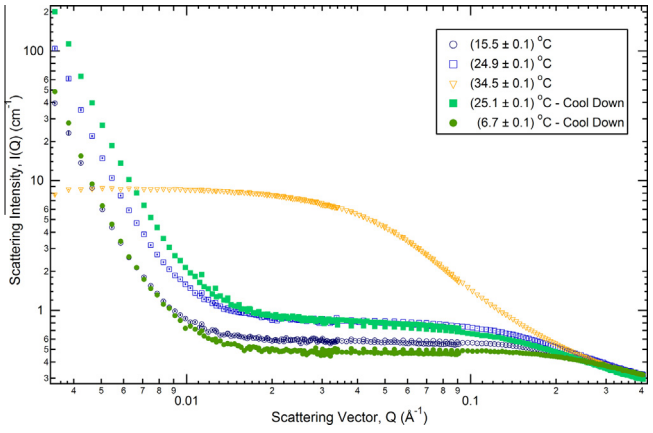

Fig. 7. SANS data as the $\omega = 0.23$ 17R4/D_2O sample was heated to 44.0 °C and then cooled back to 25.1 °C, then to 6.7 °C. Heating data at 15.5 °C and 24.9 °C are in region I, and data at 34.5 °C are in region II. Cooling data are in region I.

DLS indicated that unimers are still present in solution in region II ($R_h \sim 6$ Å), but the SANS data did not show unimers in region II. The unimer scattering was obscured because it would have been within the Porod regime of the micelle scattering and thus hidden by the micelle scattering.

3.3.2. Reversibility of structure formation

To test the reversibility of the copolymer aggregation, the $\omega = 0.23$ 17R4/D_2O solution was heated from region I, through region II, and into region III and then cooled back to region I (Fig. 7). The SANS data discussed in Section 3.2.1 were taken on heating at (15.5, 24.9, and 34.5) °C in region I. Then the sample was heated to 44.0 °C in region III and held at that temperature for about 7 h, whereupon it separated into two phases. Next the sample was cooled to 25.1 °C in region I and equilibrated for one hour. No signs of separate phases persisted, as would have been indicated by a structure factor peak (see Section 3.4), micelles from region II did not persist, and clusters reformed. Thus the formation of clusters in region I, of micelles in region II, and of two phases in region III are all reversible on a time scale of hours and with slight hysteresis.

3.3.3. Summary for region II

In region II, the 17R4 copolymers in D_2O solution no longer form the very large clusters seen in region I, but instead assemble reversibly into micelles that are about 30 Å in dimension. Unimers coexist with the micelles. Zero-shear viscosities in region II are 18% lower than in region I, supporting the picture of smaller assemblies of copolymers in region II. The small size of the micelles and values of the Porod exponents indicate that these are flower micelles.

3.4. Structure in region III

The only SANS data that we obtained in the two-phase region III are shown in Fig. 3 ($\omega = 0.11$) and Fig. 5 ($\omega = 0.0095$), both at 49.5 °C. The neutron beam sampled both phases and we were unable to probe the phases separately. Both samples show the strong low-Q scattering that indicates the presence of large clusters in at least one phase. Both samples also show scattering peaks at mid-Q (0.08 $Å^{-1}$) that are typical of inter-micellar interactions or correlations [15,35]. The expected higher-Q shoulders on the peaks were not observed, which can happen in polydisperse systems because polydispersity tends to smear the data by leveling peak features. We have no information on the presence of unimers in the coexisting phases because the interaction peak is at the same Q at which unimers would scatter.

Recall that the cloud point curve in Fig. 1 is not the same as a true coexistence curve. The true coexistence curve for 17R4 in D_2O at 49.5 °C shows a tieline for which the higher concentration upper phase has $\omega \sim 0.5$ and the lower phase has $\omega \sim 0.03$ [1]. The lever rule indicates that the upper phase is the smaller phase in both samples, at about 15% of the $\omega = 0.11$ sample and still less for the $\omega = 0.0095$ sample (which is hard to assess due to uncertainties in that region of the coexistence curve).

Thus we would hypothesize that the larger, lower phase is in region I and that it can contain large clusters (Fig. 4). These clusters would cause the low-Q scattering. We would expect the smaller, upper phase to be in region II and contain flower micelles and unimers. However, the upper phase is very concentrated, so it is also possible that the crowded micelles have formed the kind of micellar network seen in 25R8, in which the micelles share strands of the copolymer unimers [31,35]. Such a network would scatter at low Q, like the clusters, making it difficult to assess if the scattering at low Q is due to clusters of unimers, a micellar network, or both.

4. Conclusion

Our study of the solutions of the triblock copolymer 17R4, PPO_{14}–PEO_{24}–PPO_{14}, in the solvent D_2O by rheometry, DLS, and SANS has led to further understanding of the self-assembly of the copolymer in the three regions of the phase diagram (Fig. 1) [1]. At the lowest temperatures and mass fractions in one-phase region I, the copolymer exists as free polymer chains (unimers) with radii of gyration of less than 10 Å. At higher mass fractions and temperatures in region I, very large clusters are formed (larger than 200 Å) that coexist with the unimers. Such clusters cause the cloudiness seen in region I of 17R4 in H_2O [2] and in D_2O. Above the micellization line in the one-phase region II, the large clusters disappear and small (~30 Å) flower micelles develop. Unimers coexist with the micelles. In region III, above the lower critical solution point, the solution separates into two coexisting liquid phases. We could not assess the presence of unimers in region III. At 49.5 °C, the upper, more concentrated phase is in region II and contains micelles and perhaps a crowded micellar network. The lower, less concentrated phase is in region I and contains clusters.

We observed that over long times (weeks) in region I, a gel-like opaque layer formed at the liquid–air interface. The slow formation of this layer could indicate long equilibration times in the system, but all other indications were that the structure formation and the phase separation happen within an hour or two, and readily reverse within an hour or two. This surface film has not been reported previously and is worth further examination.

Our work on 17R4 in D_2O was motivated by the work of Zhou and Chu on 17R4 in H_2O using viscometry and light scattering [2]. In region I, Zhou and Chu found unimers of about 10 Å, but they did not observe large clusters or surface films for 17R4 in H_2O. In region II, they observed micellar structures with hydrodynamic radii of about 40 Å and micellization numbers of about 10. Thus the two systems are similar in forming small micelles in region II. While Zhou and Chu were not able with their probes to observe the large clusters in region I and in region III, it is likely that the cloudiness that they did see was due to such large assemblies. H_2O and D_2O are not the same solvent, because hydrophobic effects and hydrogen bonding are stronger in D_2O than in H_2O [24–26]. We would expect the incompatibility of PPO to be greater in D_2O than in H_2O, hence the even smaller micelles in D_2O in region II, and even larger clusters in region I. The formation of flower micelles by triblock copolymers like 17R4 with insoluble end blocks has been a controversial issue [5,6,36]. Our results add to the experimental data on systems that do form flower micelles [3,5,37–40].

Acknowledgments

The authors acknowledge the donors of the Petroleum Research Fund, administered by the American Chemical Society, for their support of this research. The authors thank Srinivasa R. Raghavan for the use of his DLS instrument and Donald T. Jacobs for helpful discussions. The authors acknowledge support of the National Institute of Standards and Technology, U.S. Department of Commerce, for providing the neutron research facilities used in this work. This work is based upon activities supported in part by the National Science Foundation under Agreement No. DMR-0944772. The identification of commercial products does not imply recommendation or endorsement by the National Institute of Standards and Technology, nor does it imply that these are the best available for the purpose.

Appendix A. Supplementary material

Supplementary data associated with this article can be found, in the online version, at http://dx.doi.org/10.1016/j.jcis.2014.07.049.

References

[1] A. Huff, K. Patton, H. Odhner, D.T. Jacobs, B.C. Clover, S.C. Greer, Langmuir 27 (2011) 1707.
[2] Z. Zhou, B. Chu, Macromolecules 27 (1994) 2025.
[3] B. Chu, T. Liu, C. Wu, Z. Zhou, Macromol. Symp. 118 (1997) 221.
[4] R. Koningsveld, W.H. Stockmayer, E. Nies, Polymer Phase Diagrams, Oxford University Press, Oxford, 2001.
[5] N.P. Balsara, M. Tirrell, T.P. Lodge, Macromolecules 24 (1991) 1975.
[6] M. Nguyen-Misra, W.L. Mattice, Macromolecules 28 (1995) 1444.
[7] B.C. Clover, The University of Maryland (Ph. D. dissertation), College Park, 2010. Note: Please see the Supplementary Information (Table S4) for corrected index tables from this reference.
[8] J.R. Heiks, M.K. Barnett, L.V. Jones, E. Orban, J. Phys. Chem. 58 (1954) 488.
[9] D. Prokie, J. Phys. E: Sci. Instrum. 15 (1982) 282.
[10] C.D. Ploetz, S.C. Greer, Langmuir 25 (2009) 13402.
[11] C.D. Ploetz, University of Maryland (Ph. D. dissertation), College Park, 2008.
[12] H. Odhner, D.T. Jacobs, J. Chem. Eng. Data 57 (2012) 166.
[13] M.A. Anisimov, Personal Communication.
[14] C.J. Glinka, J.G. Barker, B. Hammouda, S. Krueger, J.J. Moyer, W.J. Orts, J. Appl. Crystallogr. 31 (1998) 430.
[15] B. Hammouda, Probing Nanoscale Structures: The SANS Toolbox, <http://www.ncnr.nist.gov/staff/hammouda/the_SANS_toolbox.pdf>, 2010.
[16] S.M. King, in: R.A. Pethrick, J.V. Dawkins (Eds.), Modern Techniques for Polymer Characterisation, John Wiley and Sons, Ltd., New York, NY, 1999, p. 171.
[17] G. Porod, Kolloid Zeit. 124 (1951) 83.
[18] G. Porod, Kolloid Zeit. 125 (1952) 51.
[19] S.R. Kline, J. Appl. Crystallogr. 39 (2006) 895.
[20] B. Hammouda, J. Appl. Cryst. 43 (2010) 716.
[21] B. Hammouda, D. Ho, S. Kline, Macromolecules 35 (2002) 8578.
[22] M.G. Munoz, F. Monroy, F. Ortega, R.G. Rubio, D. Langevin, Langmuir 16 (2000) 1083.
[23] M.G. Munoz, F. Monroy, F. Ortega, R.G. Rubio, D. Langevin, Langmuir 19 (2003) 1094.
[24] A. Engdahl, B. Nelander, J. Chem. Phys. 86 (1987) 1819.
[25] C.H. Luan, D.W. Urry, J. Phys. Chem. 95 (1991) 7896.
[26] P. Mukerjee, P. Kapauan, H.G. Meyer, J. Phys. Chem. 70 (1966) 783.
[27] B. Hammouda, Polymer 50 (2009) 5293.
[28] B. Hammouda, D. Ho, S. Kline, Macromolecules 37 (2004) 6932.
[29] D. Ho, B. Hammouda, S. Kline, J. Polym. Sci. Polym. Phys. Ed. 41 (2003) 135.
[30] F. Horkay, B. Hammouda, Colloid Polym. Sci. 286 (2008) 611.
[31] K. Mortensen, W. Brown, E. Jorgensen, Macromolecules 27 (1994) 5654.
[32] Z. Zhou, B. Chu, Macromolecules 21 (1988) 2548.
[33] L. Yang, P. Alexandridis, D.C. Steytler, M.J. Kositza, J.F. Holzwarth, Langmuir 16 (2000) 8555.
[34] B. Naskar, S. Ghosh, S.P. Moulik, Langmuir 28 (2012) 7134.
[35] K. Mortensen, Polym. Adv. Technol. 12 (2001) 2.
[36] G. ten Brinke, G. Hadziioannou, Macromoleculles 20 (1987) 486.
[37] Z. Zhou, Y.-W. Yang, C. Booth, B. Chu, Macromolecules 29 (1996) 8357.
[38] T. Liu, Z. Zhou, C. Wu, B. Chu, D.K. Schneider, V.M. Nace, J. Phys. Chem. B 101 (1997) 8808.
[39] T. Liu, K. Kim, B.S. Hsiao, B. Chu, Polymer 45 (2004) 7989.
[40] F.C. Giacomelli, I.C. Riegel, C.L. Petzhold, N.P. daSilveira, P. Stepanek, Langmuir 25 (2009) 3487.